Journal of Alloys and Compounds 520 (2012) 127–131

Contents lists available at SciVerse ScienceDirect

Journal of Alloys and Compounds

journal homepage: www.elsevier.com/locate/jallcom

Effective preparation of SiC nanoparticles by the reaction of thermal nitrogen plasma with solid SiC

Hideo Okuyama[a], Sho Saito[a,b,1], Masahiro Uda[a], Takeshi Nakata[b], Yoshio Sakka[a,*]

[a] National Institute for Materials Science, 1-2-1 Sengen, Tsukuba-shi, Ibaraki 305-0047, Japan
[b] Shibaura Institute of Technology, 3-7-5 Toyosu, Kotoh-ku, Tokyo 108-8548, Japan

ARTICLE INFO

Article history:
Received 10 May 2010
Received in revised form
28 December 2011
Accepted 29 December 2011
Available online 13 January 2012

Keywords:
SiC
Nanoparticles
Arc plasma
Nitrogen gas

ABSTRACT

It is well known that SiC nanoparticles are mainly prepared by a gas phase reaction involving thermal decomposition or by precursor methods. In this paper, we propose a new process of effectively preparing SiC nanoparticles through a reaction between nitrogen arc plasma and a solid SiC block or a mixture compact of Si and C powders. The solid SiC block is irradiated with nitrogen arc plasma containing various nitrogen partial pressures at a total pressure of 0.1 MPa. The generation rate of SiC nanoparticles in 100% Ar plasma is negligible. However, the generation rate of SiC nanoparticles increases with increasing the nitrogen concentration in Ar. In the case of 100% nitrogen plasma, the generation rate has the highest value.

1. Introduction

SiC is widely used as refractory materials, disc brakes, filter materials, cutting tools, catalyst support, and heater materials because of its superior properties, which include high fracture strength, excellent creep and wear resistances, high hardness, heat resistance at high temperatures, corrosion resistance at high temperatures, and abrasion resistance [1–3]. Recently, SiC has been used both in high-temperature heating and in the fabrication process of silicon wafers, which are critical to the semiconductor industry, and is being actively studied with the aim of achieving high-purity and large-scale production [1,2].

Since Prochazka's [4] discovery that the addition of both boron and carbon improves the sintering resistance, the development of sintering aids has progressed, for example, in the recent study of Al_3BC_3 by Tanaka et al. [5,6] For application to silicon industry, however, high-purity SiC and pressure sintering such as hot pressing, spark plasma sintering, etc. [1,7,8] are required. Meanwhile, to produce high-purity SiC without sintering aids the gas-phase [9–13] and precursor methods [14–18] have mainly been studied to produce high-purity and fine-particle SiC. In the gas-phase method especially, fine-particle SiC production via reaction processes such as plasma CVD is well known with the raw materials of silicon tetrachloride and methane, and silane and methane [12].

We have successfully prepared metal [19,20], ceramic [21,22], mixed metal and ceramic [23,24] and composite nanoparticles [25–27], by the application of DC arc plasma. We are also developing an efficient method for producing nanoparticles and are achieving to understand their preparation mechanisms. For preparation of SiC nanoparticles [21], we have reported a method in which DC arc plasma in an Ar atmosphere containing H_2. However, its production mechanism and moreover, an efficient production process for this method have not been established. Here, the efficient preparation of SiC nanoparticles in an N_2 atmosphere is reported. The identification of the formation phase, particle size and shape, and the particle formation mechanism are studied for the SiC nanoparticles obtained. This approach significantly differs from traditional CVD methods, and has the following features; (1) the starting material is a solid block-like material, instead of a gas; (2) the gas component of the DC arc plasma atmosphere is the mixed gas of Ar and N_2; and (3) the N_2 gas is essential for the efficient production of SiC nanoparticles.

2. Experimental

2.1. Experimental apparatus

Fig. 1 shows a schematic diagram of the apparatus used for the study of preparing nanoparticles. The apparatus is composed of (1) a nanoparticle generator system; (2) a power supply for the DC arc discharge system; (3) a trap for the nanoparticles system; (4) a gas circulator system; (5) a gas supply system; and (6) vacuum system.

---

[*] Corresponding author. Tel.: +81 29 859 2461; fax: +81 29 859 2401.
E-mail address: SAKKA.Yoshio@nims.go.jp (Y. Sakka).
[1] Present address: Ibiden Co., Ltd.

0925-8388/$ – see front matter © 2012 Elsevier B.V. All rights reserved.
doi:10.1016/j.jallcom.2011.12.149

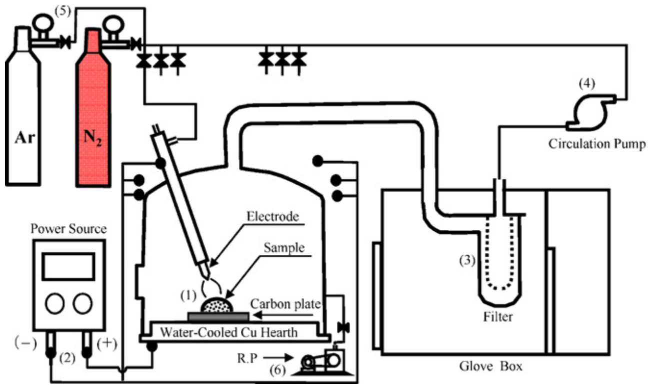

Fig. 1. Apparatus used for preparing the SiC nanoparticles by nitrogen plasma irradiation.

(1) *Nanoparticle generator system*: In principle, this is a DC arc furnace with an arc discharge. Thus, it consists of a tungsten electrode (−) paired with a water-cooled copper pedestal (+). The target material is set on the water-cooled copper pedestal, and the DC arc discharge between the target (+) and the tungsten electrode (−) converts the target to nanoparticles. The states of generated nanoparticles are greatly affected by both the gas type and the partial pressure of the atmosphere, and our previous study revealed that the target material (generally metal) is extremely easy to evaporate (i.e., easy to turn into nanoparticles) through discharge, particularly in an atmosphere containing H_2 and N_2 gases, which are diatomic molecules [21–25].

In this experiment, SiC or a mixture of Si and C is used as the raw material of the nanoparticles, and Ar gas containing N_2 or 100 vol.% N_2 gas is used as the atmosphere; the production of SiC nanoparticles is performed through the application of DC arc discharge at the total pressure of 0.1 MPa.

(2) *Power supply for the DC arc discharge system*: This is designed to stabilize the discharge state, even for different types of gas (welding power supply was not available). The discharge voltage is 10–30 V for Ar and 30–75 V for H_2 and N_2.

(3) *Trap for nanoparticles system*: The nanoparticles produced in (1) are transferred into a trapping section along with the gas flow created by the atmosphere, and then accumulate in a collection filter (stainless steel filter, 3 μm pore, Nippon Seisen Co, Ltd.) which is installed in a glove box so that collected nanoparticle could be handled in an inert gas atmosphere.

(4) *Gas circulation system*: N_2–Ar or N_2 atmosphere after trapping nanoparticle is returned the nanoparticle generator by circulation pump.

(5) *Gas supply system*: After raw material is placed on a water-cooled copper hearth (+), the apparatus is evacuated by rotary pump to 1 Pa and then back filled with N_2–Ar or N_2 atmosphere to 0.1 MPa.

2.2. Raw material

Two types of raw material were prepared for the production of SiC nanoparticles. One is massive SiC (Kojundo-Kagaku Co., Ltd., above 99.99% purity) and the other was a mixture compact of Si and C powders. Mixed compacts, consisting of Si-powder (Kojundo-Kagaku 99.9% purity, 150 μm particle size) and C powder (Kojundo-Kagaku 99.9% purity, 50 μm particle size) with the same molar ratio were formed in a uniaxial press.

2.3. Preparation conditions

Nanoparticles of SiC were produced by arc plasmas in the conditions of 100% Ar, 25% N_2–Ar, 50% N_2–Ar, 75% N_2–Ar and 100% N_2 at 0.1 MPa pressure. The current fixed 150 A, and the voltage was varied according to N_2 gas components and was increased to 25–75 V depending on the N_2 concentration in Ar. The conditions for nanoparticle production are summarized in Table 1.

SiC is a semiconductor material at room temperature and does not exhibit electrical conductivity. The raw materials used for nanoparticle production (+) was loaded on the carbon crucible, and arc plasma was initially irradiated onto the crucible; irradiation of the nanoparticle material (+) was performed via an indirect heating process, which was also effective in preventing the dispersal of the material by plasma thermal shock due to rapid heating.

2.4. Characterization

Phase identification of the produced nanoparticles was performed by X-ray diffraction via CuKα-ray. The morphology was observed achieved by transmission electron microscopy (TEM) with a 200 kV accelerating voltage. To prepare the sample for observation, the powder was dispersed in ethanol by ultrasound, and droplets were set on the copper mesh with corrosion film. In terms of size, the average particle-size was calculated from surface area measurement based on the BET method.

Table 1
Experimental conditions of nitrogen plasma irradiation on SiC and mixtured compact of Si and C powders.

Parameters	Value
Volume	≒ 3.5 cm^3
Gases in atmosphere	100% Ar
	25% N_2–Ar
	50% N_2–Ar
	75% N_2–Ar
	100%N_2
Pressure in atmosphere	0.1 MPa
Arc voltage	25–75 V
Arc irradiation time	2–3 min

3. Results and discussion

3.1. Production of SiC nanoparticles by the irradiation of Ar plasma

When massive SiC were chosen as the raw material, there was no change in the shape of the material before and after Ar plasma irradiation, and nanoparticles formation was not observed in the Ar atmosphere. In the case of a mixed compact of Si and C powders, the compact was shrank due to the reaction of the melted Si and C powders (SiC formation), but the formation of SiC nanoparticles was still not observed in the Ar atmosphere.

The result of X-ray diffraction for the mixed compact of Si and C powders after the irradiation of Ar plasma is presented in Fig. 2, which shows some peaks from the SiC, Si and C.

From chemical analysis, the concentration (wt%) of Si and SiC in mixed compact after Ar plasma irradiation is known to be 0.38% Si and 99% SiC. From the results above, it is clear that the mixed compact of Si and C by irradiation of Ar plasma is change to the materials of 99% SiC and Si (below 1%).

3.2. Production of SiC nanoparticles by the irradiation of nitrogen plasma

Although SiC nanoparticle production was not observed when Ar plasma was irradiated on the starting material of massive SiC, a smoke like vapor was initially observed when nitrogen plasma was irradiated on massive SiC. A photograph of SiC nanoparticles produced by the irradiation of nitrogen plasma shows in Fig. 3(a), and a schematic diagram of nanoparticle production is shown in Fig. 3(b). As illustrated in Fig. 3, the SiC vapor (nanoparticles formed

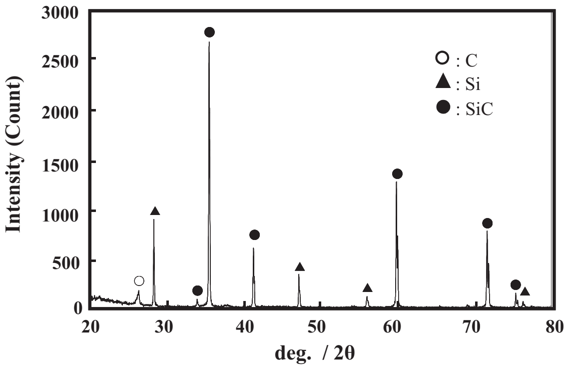

Fig. 2. X-ray diffraction pattern for mixed compact of Si and C powders after irradiating Ar plasma.

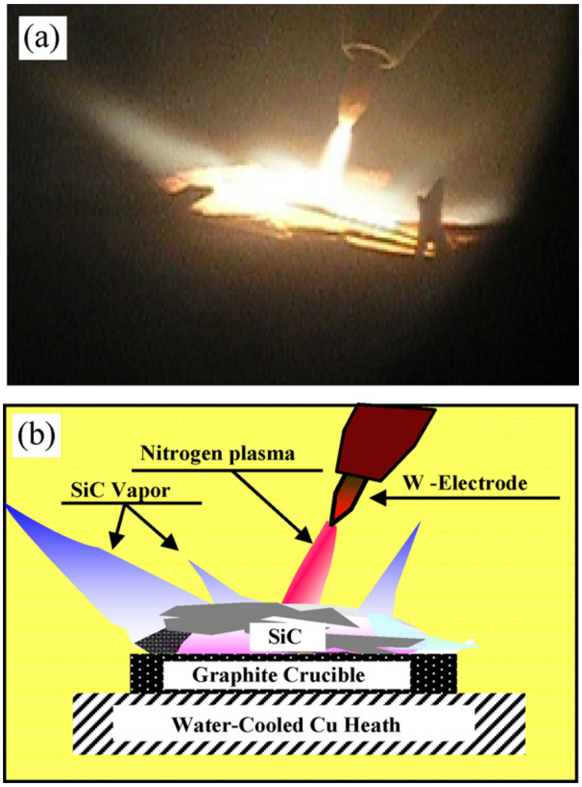

Fig. 3. (a) Photograph of SiC nanoparticles generated from the SiC material by radiation with nitrogen plasma. (b) Sketch diagram of SiC nanoparticles generated from SiC material by radiation with nitrogen plasma.

from condensed vapor) is created just around the place where the N plasma is irradiated.

From the difference between the mass of the material before and after nitrogen plasma irradiation, the rate of SiC nanoparticle production was calculated. Fig. 4 shows the relationship between N_2 concentration (vol.%) in Ar–N_2 atmospheres and the rate of SiC nanoparticle production. The production rate increased with increasing the N_2 concentration. Thus, nitrogen plasma contributes significantly to SiC nanoparticle production. The production rate is highest (about 80 g/h) at 100 vol.% N_2.

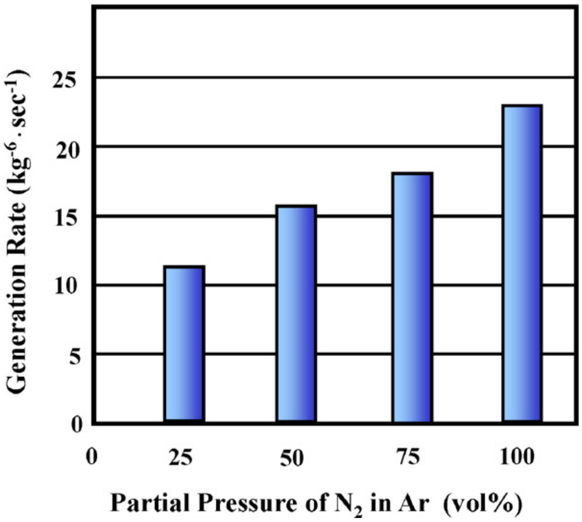

Fig. 4. Rate of generation of nanoparticles created by irradiating nitrogen plasma on SiC.

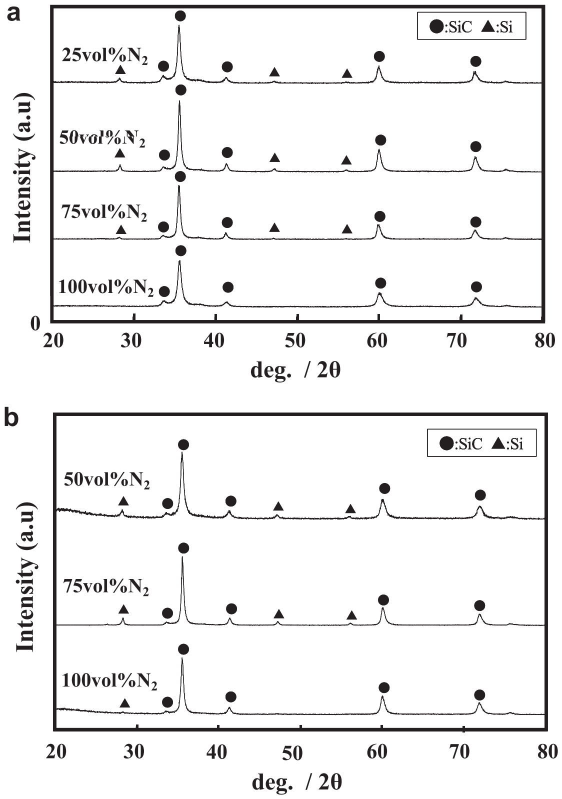

Fig. 5. X-ray diffraction patterns of nanoparticles prepared by irradiating on (a) SiC (a) and (b) compact Si and C powders with nitrogen plasma.

The X-ray diffraction patterns for nanoparticles with various N_2 concentration in Ar gas are presented in Fig. 5. The raw material of SiC is in Fig. 5(a), and the mixed-materials of Si- and C-powder is in Fig. 5(b). As shown in Fig. 5(a) and (b), neither of the initial materials makes a significant difference at the production phase, and it is clear that both of the materials make almost the same phase nanoparticles. In particular, at 100 vol.% N_2 density, shown in Fig. 5(a), the impurity phase of Si is not observed, and hence the SiC nanoparticles that have been produced are single phase. In Fig. 5(b), it is clear that a lesser amount of the impurity phase is also seen with 100 vol.% N_2 density.

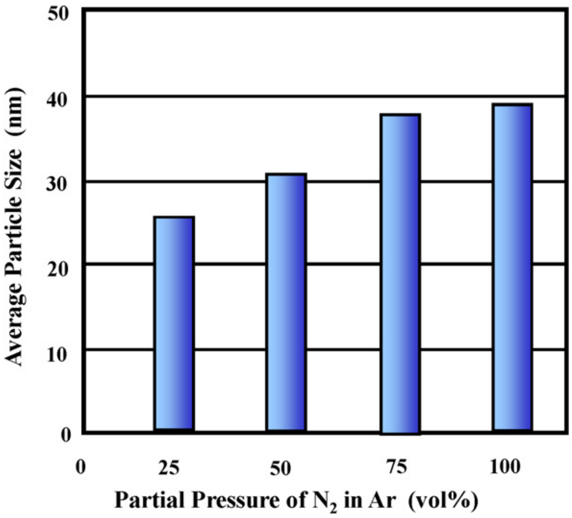

Fig. 6. Average particle size of nanoparticles created by irradiating plasma with SiC under different partial pressures of N_2 in Ar.

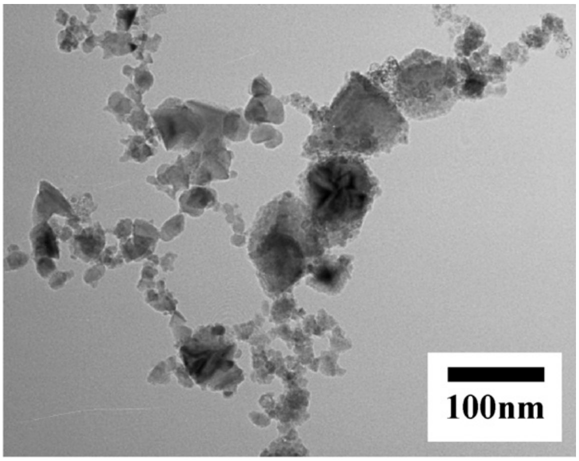

(a) 50 vol% N_2-Ar

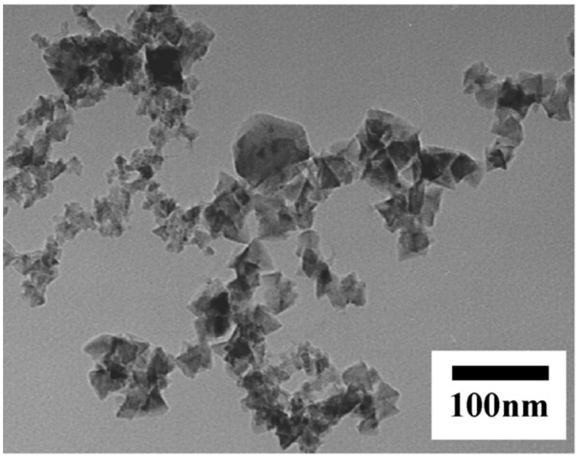

(b) 100 vol% N_2

Fig. 7. TEM micrographs of nanoparticles created by irradiating arc plasmas on SiC in 50 vol.% N_2–Ar (a) and 100 vol.% Ar (b) atmosphere at 0.1 MPa pressure.

The color of the SiC nanoparticles that were produced was a deep dark green. Fig. 6 presents the average particle-sizes, from surface-area measurement, with various N_2 densities in atmosphere. As the figure shows, there is a tendency for the average particle-size to become larger according to an increase of N_2 density in atmosphere.

TEM images of the produced nanoparticles in atmosphere, which are composed of 50 vol.% N_2–Ar and 100 vol.% N_2, are shown in Fig. 7(a) and (b), respectively. In terms of particle-size, there is no significant difference between them. The nanoparticle size was distributed in the range of 20–100 nm. This result is quite consistent with the average particle size (30–40 nm) in Fig. 6. In addition, it is known that, in the crystal structure of SiC, there are many different forms that share vertices of a tetrahedron [1,28,29]. Various types of polygonal forms, mainly tetrahedrons, were observed in the nanoparticles produced by this method.

3.3. Discussion on the form of SiC nanoparticle crystals

SiC is known to exhibit many types of polymorphism, depending on the number of layers; and cube-shaped crystals are categorized as β-SiC (3C), while crystals of other shapes are α-phase (2H, 4H, 6H...) [1]. From the XRD and ICDD card in Fig. 5, the produced nanoparticle is indicated to have a structure close those of 3C and 6H, but a clear decision could not be made with the results obtained from the X-ray diffraction because of the broadness of the bandwidth. The reasons of for the broadness of the X-ray diffraction are thought to be the small particle-size and stacking faults that occur due to the rapid cooling from an ultra-high temperature in the plasma stage. Therefore, the nanoparticles that were produced might have different crystal structure shapes, mainly 3C and 6H. In addition to the X-ray diffraction, the TEM images in Fig. 7(a) and (b) also shows that the nanoparticles have various shapes. Therefore, it is estimated that the SiC nanoparticle exhibits many types of polymorphism.

In relation to the production of metal nanoparticles, we have so far clarified that various metals and alloys can easily be evaporated by the application of DC arc plasma in atmospheres containing diatomic molecular gases such as H_2, N_2 and that the evaporation rate increases exponentially with increasing of H_2 or N_2 concentration in the atmosphere; as a result, the production rates of metal and alloy nanoparticles rise markedly. The reason for this is, the activity of atomic H or N, which is are significantly a higher than that of molecular H_2 or N_2 and a large amount of H or N is dissolved into the molten metal (super saturated of H or N) However, this supersaturated state is extremely unstable for the non-arc atmosphere (molecular H_2 or N_2 gas phase) and the excess part of super-saturated H or N is ejected as corresponding molecular gas from the molten metal to the outside of arc plasma flame. The metal atoms might be emitted at the same time as the H_2 or N_2 gas is evolved. Similar formation mechanism of SiC nanoparticles is considered that the behavior of the N_2 gas, both in terms of dissolution and release, induce the forced-evaporation of SiC as is the case of metal [19–21].

4. Conclusions

It has been revealed that the production of SiC nanoparticles was efficiently performed by the application of DC arc plasma irradiation of Ar–N_2 mixed-gas under the atmospheric pressure. The SiC nanoparticle production rate increased with increasing N_2 concentration in the mixed gas, and the highest production rate attained was about 80 g/h at 100 vol.% N_2 concentration. In the case of 100% Ar plasma, the SiC nanoparticle production rate was too small to be measured.

Therefore, our nanoparticle production method is completely different from other method involving sublimation (evaporation) of SiC by heating to high temperatures.

References

[1] H.S. Tanaka, J. Ceram. Soc. Jpn. 119 (2011) 218–233.
[2] A. Somiya, Y. Inomata (Eds.), Silicon Carbite Ceramics-2, Elsevier Science Publishers Ltd., Barking, England, 1991.
[3] B. Ghosh, S.K. Pradhan, J. Alloys Compd. 486 (2009) 480–485.
[4] S. Prochazka, R.M. Scanlan, J. Am. Ceram. Soc. 58 (1975) 72.
[5] H. Tanaka, N. Hirosaki, N. Nishimura, J. Ceram. Soc. Jpn. 111 (2003) 878–882.
[6] S.H. Lee, Y. Sakka, H. Tanaka, Y. Kagawa, J. Am. Ceram. Soc. 92 (2009) 2888–2893.
[7] S. Grasso, Y. Sakka, G. Maizza, Sci. Technol. Adv. Mater. 10 (2009) 053001.
[8] Z.A. Munir, D.V. Quach, M. Ohyagi, J. Am. Ceram. Soc. 94 (2011) 1–19.
[9] Y.S. Suyama, R.M. Marra, J.S. Haggerty, H.K. Bowen, Am. Ceram. Soc. Bull. 64 (1985) 1356–1359.
[10] Y. Okabe, J. Hojo, M. Kato, Nippon Kagaku Kaishi (1980) 188–193.
[11] Y. Ando, R. Uyeda, J. Cryst. Growth 52 (1981) 178–181.
[12] C.M. Hollabaugh, D.E. Hull, L.R. Newkirk, J.J. Petrovic, J. Mater. Sci. 18 (1983) 3190–3194.
[13] Q. Pang, L. Xu, Z. Ju, L. Yang, Q. Hao, Y. Qian, J. Alloys Compd. 501 (2010) 60–66.
[14] R. Riedel, G. Mera, R. Hauser, A. Kionczynski, J. Ceram. Soc. Jpn. 114 (2006) 425–444.
[15] H. Tanaka, Y. Kurachi, Ceram. Inter. 14 (1988) 109–115.
[16] S. Ishihara, H. Tanaka, T. Nishimura, J. Mater. Res. 21 (2006) 1167–1174.
[17] Y. Yoshioka, M. Konishi, H. Tanaka, T. Nishimura, Y. Sakka, J. Ceram. Soc. Jpn. 118 (2010) 345–348.
[18] N. Najafi, F. Golestani-Fard, H.R. Rezaie, N. Ehsani, J. Alloys Compd. 505 (2010) 692–697.
[19] S. Ohno, M. Uda, J. Jpn. Inst. Met. 48 (1984) 640–646.
[20] S. Ohno, M. Uda, J. Jpn. Inst. Met. 53 (1989) 946–952.
[21] S. Ohno, M. Uda, H. Okuyama, J. Soc. Powder Technol. Jpn. 21 (1984) 747–752.

[22] Y. Sakka, S. Ohno, M. Uda, J. Am. Ceram. Soc. 75 (1992) 244–248.
[23] Y. Sakka, S. Ohno, Nanostruct. Mater. 7 (1996) 341–353.
[24] Y. Sakka, H. Okuyama, T. Uchikoshi, S. Ohno, Nanostruct. Mater. 5 (1995) 577–588.
[25] Y. Sakka, H. Okuyama, T. Uchikoshi, S. Ohno, J. Alloys Compd. 346 (2002) 285–291.
[26] K. Kitawaki, K. Kaneko, K. Inoke, J.C. Hernandez-Garrido, P.A. Midgley, H. Okuyama, M. Uda, Y. Sakka, Micron 40 (2009) 308–312.
[27] K. Kaneko, K. Kitawakia, S. Sadayama, H. Razavi, J.C. Hernandez-Garrido, P.A. Midgley, H. Okuyama, M. Uda, Y. Sakka, J. Alloys Compd. 492 (2010) 685–690.
[28] G. Sasaki, K. Hiragi, M. Hirabayashi, K. Niihara, T. Hirai, J. Ceram. Soc. Jpn. 94 (1986) 779.
[29] Y.C. Zhou, F. Xia, J. Am. Ceram. Soc. 74 (1991) 447–449.